

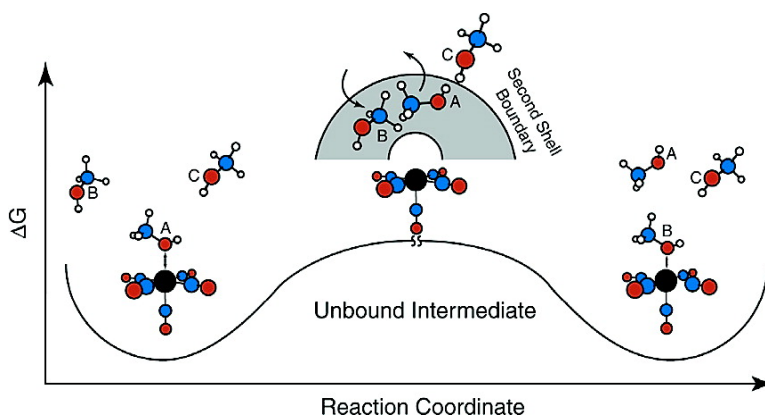
Article

## Mechanism of Ligand Exchange Studied Using Transition Path Sampling

Preston T. Snee, Jennifer Shanoski, and Charles B. Harris

*J. Am. Chem. Soc.*, **2005**, 127 (4), 1286-1290 • DOI: 10.1021/ja044807t • Publication Date (Web): 08 January 2005

Downloaded from <http://pubs.acs.org> on March 24, 2009



### More About This Article

Additional resources and features associated with this article are available within the HTML version:

- Supporting Information
- Links to the 4 articles that cite this article, as of the time of this article download
- Access to high resolution figures
- Links to articles and content related to this article
- Copyright permission to reproduce figures and/or text from this article

[View the Full Text HTML](#)

## Mechanism of Ligand Exchange Studied Using Transition Path Sampling

Preston T. Snee,<sup>†</sup> Jennifer Shanoski, and Charles B. Harris\*

Contribution from the Department of Chemistry, University of California, Berkeley, California 94720, and Chemical Sciences Division, Ernest Orlando Lawrence Berkeley, National Laboratory, Berkeley, California, 94720

Received August 27, 2004; E-mail: harris@socrates.berkeley.edu

**Abstract:** The mechanism of intermolecular ligand exchange has been studied using transition path sampling (TPS) based molecular dynamics (MD) simulations. Specifically, the exchange of solvent molecules bound to unsaturated Cr(CO)<sub>5</sub> in methanol solution has been investigated. The results of the TPS simulations have shown that there are multiple steps in the reaction mechanism. The first involves partial dissociation of the coordinated solvent from the Cr metal center followed by association with a new methanol molecule between the normally void first and second solvent layers. After diffusive motion of the exchanging ligands, the last step involves the originally bound methanol molecule moving into the bath continuum followed by solvation of the Cr metal fragment by the exchanging ligand. It has been found that the reaction center (defined as the organometallic fragment and two exchanging ligands only) and the solvent bath have favorable interactions. This is likely due to the adiabatic nature of the ligand exchange transition. The ability to understand the microscopic molecular dynamics of a chemical process based on a free energy analysis is also discussed.

### I. Introduction

The dynamics of coordinatively unsaturated organometallic compounds have been the subject of intense study due to their importance in many synthetic and catalytic processes.<sup>1</sup> Research in this field has been aided by the advent of ultrafast laser spectroscopy, allowing for the unambiguous observation of the formation of products from photogenerated reactants in solution. It has been established that a coordinatively unsaturated metal center can bind to a nonreactive solvent molecule such as an alkane, which acts as a “token ligand”.<sup>2–6</sup> These results are consistent with time-resolved studies on Group 6 metal carbonyls in neat RX (R = alkyl, X = Cl, OH, etc.) solutions, in which the formation and subsequent dynamics of a loosely bound alkyl-metal intermediate species following photolysis were characterized.<sup>4,7–17</sup> The rearrangement of a relatively weakly bound alkyl-metal transient to a strongly solvated

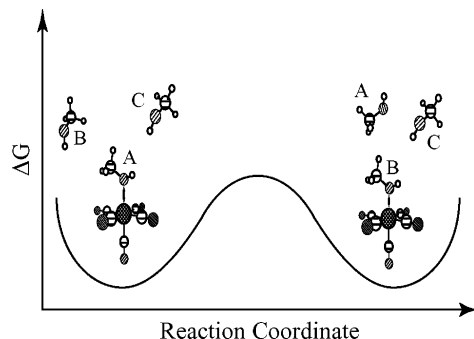
product is generally the rate limiting step in the reaction. While intermolecular ligand exchange of coordinatively saturated species is described using associative, dissociative, or interchange mechanisms,<sup>18</sup> previous investigations concluded that unsaturated metal fragments form products in a neat solvent via an intramolecular process.<sup>7,8</sup> However, recent works have shown that unsaturated organometallic intermediates exchange loosely bound “token ligands” via an intermolecular mechanism as summarized in Scheme 1.<sup>9–17</sup> At present, there is no agreement about whether this mechanism is best described as associative, dissociative, or interchange in nature. Mechanistic studies of these processes are inherently difficult with time domain spectroscopies due to the lack of a well-defined initiation step. Theoretical methods, however, do not suffer from such limitations because they are able to focus on specific, microscopic, rare events.

To address this issue, we have performed molecular dynamics (MD) simulations of intermolecular rearrangement to develop a microscopic understanding of the mechanism. The transition path sampling (TPS) method of Chandler and co-workers has been utilized to simulate intermolecular rearrangements without

<sup>†</sup> Present address: Department of Chemistry, Massachusetts Institute of Technology, 77 Massachusetts Ave., Room 18-080, Cambridge, MA 02139.

- (1) Hall, C.; Perutz, R. N. *Chem. Rev.* **1996**, *96*, 3125.
- (2) Perutz, R. N.; Turner, J. J. *J. Am. Chem. Soc.* **1975**, *97*, 4791.
- (3) Yang, G. K.; Viada, V.; Peters, K. S. *Polyhedron* **1988**, *7*, 1619.
- (4) Hu, S. N.; Farrell, G. J.; Cook, C.; Johnson, R.; Burkey, T. J. *Organometallics* **1994**, *13*, 4127.
- (5) Yang, H.; Asplund, M. C.; Kotz, K. T.; Wilkens, M. J.; Frei, H.; Harris, C. B. *J. Am. Chem. Soc.* **1998**, *120*, 10154.
- (6) Geftakis, S.; Ball, G. E. *J. Am. Chem. Soc.* **1998**, *120*, 9953.
- (7) Simon, J. D.; Xie, X. J. *Phys. Chem.* **1989**, *93*, 291.
- (8) Xie, X.; Simon, J. D. *J. Am. Chem. Soc.* **1990**, *112*, 1130.
- (9) Kotz, K. T.; Yang, H.; Snee, P. T.; Payne, C. K.; Harris, C. B. *J. Organomet. Chem.* **2000**, *596*, 183.
- (10) Zhang, S.; Zang, V.; Bajaj, H. C.; Dobson, G. R.; van Eldik, R. J. *Organomet. Chem.* **1990**, *397*, 279.
- (11) Ladogana, S.; Nayak, S. K.; Smit, J. P.; Dobson, G. R. *Organometallics* **1997**, *16*, 3051.
- (12) Ladogana, S.; Nayak, S. K.; Smit, J. P.; Dobson, G. R. *Inorg. Chem.* **1997**, *36*, 650.

- (13) Creaven, B. S.; George, M. W.; Ginzburg, A. G.; Huges, C.; Kelly, J. M.; Long, C.; McGrath, I. M.; Pryce, M. T. *Organometallics* **1993**, *12*, 3127.
- (14) Breheny, C. J.; Kelly, J. M.; Long, C.; O’Keeffe, S.; Pryce, M. T.; Russell, G.; Walsh, M. M. *Organometallics* **1998**, *17*, 3690.
- (15) Lugovskoy, A.; Paur-Afshari, R.; Schultz, R. H. *J. Phys. Chem. A* **2000**, *104*, 10587.
- (16) Krishnan, R.; Schultz, R. H. *Organometallics* **2001**, *20*, 3314.
- (17) Lugovskoy, S.; Lin, J.; Schultz, R. H. *J. Chem. Soc., Dalton Trans.* **2003**, *15*, 3103.
- (18) Cotton, F. A.; Wilkinson, G.; Gauss, P. L. *Basic Inorganic Chemistry* John Wiley and Sons: Toronto, 1995; pp 188–189.

**Scheme 1.** Process of Ligand Exchange in the Present Investigation

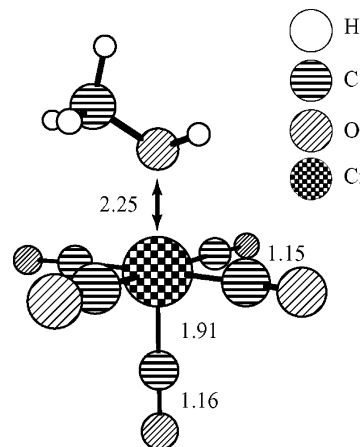
an a priori assumption of the nature of the transition state(s).<sup>19–25</sup> This technique is capable of characterizing rare molecular events such as chemical transformation and has been used to study a variety of physical phenomena.<sup>24,25</sup>

As an intermolecular mechanism appears to explain many observations of organometallic photochemistry in long chain alcohol solvents,<sup>10</sup> we have modeled the rearrangement of a strongly bound  $\text{Cr}(\text{CO})_5 \cdot (\text{OH})\text{CH}_3$  complex with another solvent molecule in neat methanol to determine the degree of the dissociative, interchange, or associative nature of the ligand exchange mechanism. The results of these simulations have revealed many of the microscopic details of the exchange mechanism as well as interesting energetic dynamics. Limiting forms of the proposed mechanism may account for previous observations made in similar systems.

## II. Methods

The purpose of these simulations is to augment previous experimental conclusions concerning the mechanism of token ligand rearrangement. We have developed a model for the interaction of a coordinatively unsaturated  $\text{Cr}(\text{CO})_5$  fragment with a methyl alcohol solvent by optimizing 15 structures of a methanol/metal complex using density functional theory (DFT). These calculations were performed using the B3LYP functional with the LACVP\*\* basis set within the JAGUAR program.<sup>26–31</sup> It can be seen from the globally optimized structure shown in Scheme 2 that the strongest interaction is between the chromium and oxygen sites. The usual Lennard–Jones and Coulombic interactions were thus augmented with bonding Morse functions between the Cr–O and Cr– $\text{CH}_3$  pairs, the parameters of which were optimized to fit the calculated theoretical interaction energies. The parameters for the potential are given in Tables 1 and 2.

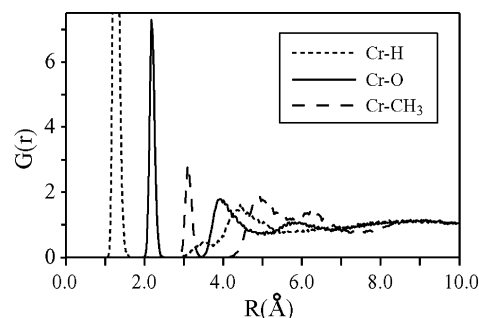
The steady-state properties of a single  $\text{Cr}(\text{CO})_5$  solute in a bath of 200 methanol molecules were calculated using classical MD techniques within the microcanonical ensemble.<sup>32,33</sup> These equilibrated simulations

**Scheme 2.** DFT Optimized Structure for the Interaction of a Single Methanol Molecule with a  $\text{Cr}(\text{CO})_5$  Fragment**Table 1.** Morse Potential Parameters for the Cr–Solvent Bonding Interactions

pair	$D_0$ (kJ/mol)	$\alpha_i$ ( $\text{nm}^{-1}$ )	$R_{\text{eq}}$ (nm)
O/Cr	66.808	18.644	2.249
$\text{CH}_3/\text{Cr}$	6.906	11.4211	2.879

**Table 2.** Lennard–Jones and Coulomb Potentials for the Molecular Dynamics Simulations

site	$q/e$	$\sigma/\text{Å}$	$\epsilon/k_b$
H	0.435	0.00	0.0
O	−0.700	3.03	105.2
$\text{CH}_3$	0.265	3.74	86.5
Cr	−0.928	N/A	0.0
$\text{C}_{\text{ax}}$	0.625	3.83	13.2
$\text{C}_{\text{eq}}$	0.655	3.83	13.2
$\text{O}_{\text{ax}}$	−0.496	3.12	80.1
$\text{O}_{\text{eq}}$	−0.456	3.12	80.1

**Figure 1.** Radial distribution functions between the Cr metal center and the methanol solvent under equilibrium conditions. The metal is solvated by a single methanol molecule.

were performed over 360 ps with an average temperature of 295 K. Shown in Figure 1 are the equilibrium Cr–H, Cr–O, and Cr– $\text{CH}_3$  pair correlation functions. The first solvent shell integrates to exactly one solvating methanol molecule, the identity of which was not observed to change over the course of these equilibrium simulations. Consequently, the exchange of the solvent ligand/ $\text{Cr}(\text{CO})_5$  complex is a rare event due to the strong interaction potential. The averages of the total reactant energy, bath/reactant coupling and reactant self-interaction energy, were calculated and compared to those observed in TPS simulations.

To characterize the molecular dynamics of the ligand exchange process with statistical significance, we have used the transition path sampling (TPS) method. First, artificial forces were added to an equilibrium simulation to create a reactive trajectory in which the

- (19) Dellago, C.; Bolhuis, P.; Chandler, D. *J. Chem. Phys.* **1998**, *108*, 9236.
- (20) Dellago, C.; Bolhuis, P.; Csajka, F.; Chandler, D. *J. Chem. Phys.* **1998**, *108*, 1964.
- (21) Dellago, C.; Bolhuis, P.; Chandler, D. *J. Chem. Phys.* **1999**, *110*, 6617.
- (22) Geissler, P. L.; Chandler, D. *J. Chem. Phys.* **2000**, *113*, 9759.
- (23) Dellago, C.; Bolhuis, P.; Chandler, D.; Geissler, P. *Annu. Rev. Phys. Chem.* **2002**, *59*, 291.
- (24) Ramirez, J.; Laso, M. *J. Chem. Phys.* **2001**, *115*, 7285.
- (25) Geissler, P. L.; Dellago, C.; Chandler, D.; Hutter, J.; Parinello, M. *Science* **2001**, *291*, 2121.
- (26) Becke, A. D. *J. Chem. Phys.* **1993**, *98*, 5648.
- (27) Lee, C.; Yang, W.; Parr, R. D. *Phys. Rev.* **1988**, *B41*, 785.
- (28) Hehre, W. J.; Ditchfield, R.; Pople, J. A. *J. Chem. Phys.* **1972**, *56*, 2257.
- (29) Francl, M. M.; Pietro, W. J.; Hehre, W. J.; Binkley, J. S.; Gordon, M. S.; Defrees, D. J.; Pople, J. A. *J. Chem. Phys.* **1982**, *77*, 3654.
- (30) Hay, P. J.; Wadt, W. R. *J. Chem. Phys.* **1985**, *82*, 299.
- (31) *Jaguar 3.5*; Schrodinger Inc.: Portland, OR, 1998.
- (32) Allen, M. P.; Tildesley, D. J. *Computer Simulations of Liquids* Clarendon Press: Oxford Science Publications: Bristol, 1987.
- (33) The energy conservation of the steady-state and TPS microcanonical simulations was generally on the order of  $\sim 0.03\%$ .

identity of the methanol solvent molecule bound to the unsaturated metal center is exchanged. Next, the artificial forces were removed, and the trajectory was annealed for several thousand reactive simulations within the transition path ensemble. This is accomplished by slightly perturbing the velocities of a single randomly selected configuration along the reactive trajectory and integrating the equations of motion both forward and backward to create a complete new path. This trial trajectory is accepted if the identity of the metal center solvating molecule has changed between the first and the last step. As the Cr–O pair potential is strong, we use the Cr–O bonding distance derived from the equilibrium pair correlation function as the criteria for the definition of a stable solvated state. If accepted, the trajectory is saved as the present working system and is analyzed for various properties. Otherwise, the trial trajectory is discarded and the process is repeated. The lengths of the trajectories were 3.9 ps, and the energies were constrained to a constant value as required within the micro-canonical ensemble. In the language of the transition path method, these “shooting” moves were accompanied with an equal number of “shifting” steps to explore the phase space of the reactive trajectories. On average, ~40% of the trial shooting trajectories were accepted and were subsequently analyzed to characterize the dynamics of the ligand exchange process.

A second series of simulations were performed to determine the nature of the potential energy surface. Approximately 4000 TPS simulations were conducted in which the initial configuration of a stable solvated state evolves into a region between the product and reactant surfaces within 3.0 ps. A 2D histogram of the nearest versus next-nearest neighbor Cr–O distances was calculated from these trajectories. Overall, there appears to be several local minima in the PES, two of which are clearly associated with the product and the reactant basins as discussed below.

### III. Results

The equilibrium radial distribution functions for the unsaturated Cr center and the solvent bath’s H, O, and CH<sub>3</sub> sites are shown in Figure 1. It can be seen that the metal fragment is strongly solvated by a single methanol molecule due to the strong Cr–OH interaction. The hydrogen site appears canted toward the metal center compared to the DFT optimized structure shown in Scheme 2, which is likely due to the inaccuracies of the classical potential surface, solvent perturbations, and the presence of long-range forces. Given the fact that the intermolecular substitution is a rare event due to the strong Cr–solvent potential, the TPS method is needed to characterize the exchange process with statistical accuracy. As the strongest bonding interaction of the solvent with the Cr atom occurs from the Cr–O bond, we define a steady-state reactant basin as having a Cr–O distance of <2.4 Å with all other molecules in the second shell and beyond. In the words of refs 19–23, the Cr–O distance is the order parameter which defines our stable reactant or product state. However, the order parameter should not be confused with the true multidimensional reaction coordinate which is very difficult to accurately characterize. The product basin has the same spatial structure as the reactant; however, the identity of the solvating molecule at the end of the simulation is not the same as that at the beginning.

Several properties of the molecular system were observed over the course of 2000 successful transitions. The results have been averaged over time with respect to the last spatial crossing of the exchanging solvent molecules, which is defined to occur at the center of the trajectory. The Cr–O distances of the exchanging methanol molecules over time are shown in Figure 2. It can be seen that the motion of the initially bound methanol

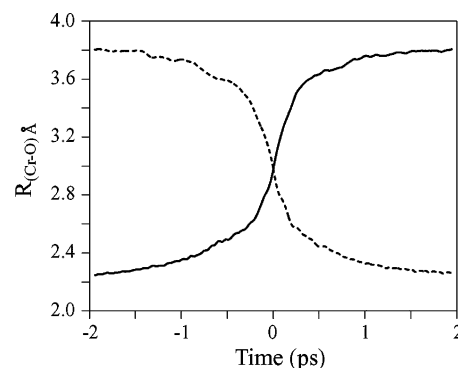


**Figure 2.** Cr–O distances during the exchange reaction. The dashed line represents the incoming ligand, and the solid line represents the motion of the originally bound methanol molecule.

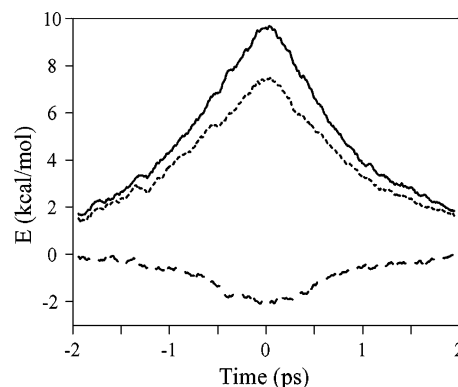


**Figure 3.** Averaged energy decomposition during the TPS simulations. Shown are the total energy of the Cr(CO)<sub>5</sub> and exchanging methanol molecules (solid line) as well as the reactive center self-energy (short dashed line). The difference is the potential energy of the reaction center with the solvent (long dashed line).

away from the metal center induces another solvent molecule to enter the normally void ( $\sim 60 \text{ \AA}^3$ ) volume between the first and second solvent shells. The system leaves this state when the formally bound methanol molecule diffuses into the second solvent shell boundary, thus allowing the exchanging molecule to fully coordinate to the metal center. This process occurs over a diffusive  $\sim 1.3$  ps time scale<sup>34</sup> but is a statistically rare event in the equilibrated ensemble. Consequently, the last step of the solvent exchange process is essentially the microscopic reverse of the first.

The dynamics of the reactant and bath energies reveal many interesting properties of the exchange process. As traditional views on the mechanism of ligand exchange focus largely on the reactive subsystem (defined as the Cr(CO)<sub>5</sub> fragment and the two nearest exchanging solvent molecules), we define the total conserved energy as

$$E = E_{\text{bath}} + E_{\text{reactant}} + V_{\text{bath/reactant}} \quad (1)$$

where  $E_{\text{reactant}}$  represents the internal metal fragment/exchanging ligands energy, while  $E_{\text{bath}}$  is the sum of the potential and kinetic energies of bath molecules only. The last term is the potential energetic coupling between the reacting molecules and the bath. Shown in Figure 3 are the reactants’ total and internal energy as well as the bath/reactant potential coupling. An interesting aspect of these data is that the bath/reactant interaction is

(34) Simulations of a neat methanol liquid show that an O site may diffuse  $\sim 1.5 \text{ \AA}$  within 1.2 ps.

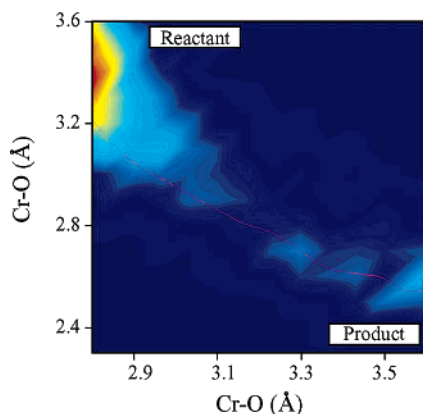


**Figure 4.** Histogram of Cr–O distances for TPS simulations that begin in the product well and end between the first and second solvent shells. There appear to be two stable states that are associated with the product and reactant basins as well as several intermediate states in between.

energetically favorable near the center of the trajectory, which results in a greater internal energy for the unsaturated metal and exchanging methanol molecules due to energy conservation within the microcanonical ensemble.

#### IV. Discussion

**A. Reaction Mechanism.** It was initially believed that the ligand exchange reaction for this model would be dissociative in nature. In this case, the coordinating solvent species would break off from the metal center of  $\text{Cr}(\text{CO})_5$  and enter into the bath continuum before another methanol molecule moved to solvate the unsaturated metal center. However, the Cr–O distances for the nearest and next nearest solvent molecules show that the exchange of solvating ligands occurs midway between the normally void first and second solvent shells as seen in Figure 2. An energy decomposition of the reaction center shows that the bonding interaction between the metal and solvating ligand is largely lost at the midpoint of the reaction. However, the metal center does gain some favorable interaction with the exchanging methanol molecule at the same time. These results suggest that  $I_d$  (dissociative interchange) mechanism is responsible for the observed dynamics. In this scheme, the reaction is assisted by the simultaneous favorable potential energy contact between the incoming and outgoing token ligands with the metal center. There also exists an energetically beneficial  $-3$  kcal/mol interaction between the exchanging methanol molecules during the exchange process.

Two possibilities exist to explain these observations. First, one or more local potential minima may connect the product and the symmetric reactant configurations. The existence of intermediate basin(s) is supported by the long time scale of ligand exchange observed in the reactive simulations. Alternatively, this observation may be the result of a long, flat potential energy surface that connects the stable product/reactant basins. To address this issue, we have performed TPS simulations from the product basin into the intermediate region where no single solvent molecule is bound to the metal center as shown in Figure 4. The results show existence of two stable basins associated with the reactant and ligand exchanged product states along with several intermediate states in between. Shown in Figure 5 are the radial distribution functions of the Cr–X ( $X = \text{H}, \text{O}, \text{CH}_3$ ) solvent sites calculated during the reactive simulations.

The solvent structure is redistributed beyond the first and second solvent layers as can be seen from the difference between the distribution functions at equilibrium and during the reaction, which suggests that large scale solvent motion is involved in the ligand exchange reaction. Overall, the results suggest that the time scale for the ligand exchange reaction is due to a highly complex multidimensional potential surface with several local minima that connects the product to the reactant states. These intermediate basins may be associated with bulk solvent reorganization that assists the exchange process.

Due to the well defined order of solvent motions into long-lived intermediate states, the  $I_d$  mechanism observed in these simulations is best described using a two-step process. The observed dynamics has dissociative character in that the coordinated solvent must initially detach from the metal center and move between the first and second solvent layer. Only after the original solvating ligand moves out of the first solvent shell can another solvent molecule diffuse into the same region. Thus while the first step has dissociative character, this second step has an associative nature. Previous studies that suggested a spectrum of reaction dynamics are more likely limiting forms of the generalized mechanism proposed below. Our observations are also similar to those made in a recent report which proposed the possibility of associative and dissociative processes operating simultaneously.<sup>17</sup> These workers also concluded that an  $I_d$  mechanism is best suited to characterize their ligand exchange studies. Note that our conclusions are not based upon the averaging of the dynamics of disparate dissociative and associative single trajectories; individual analysis of each single trajectory does not conform to either of these mechanistic descriptions.

The ligand exchange dynamics may be summarized as follows. The  $\text{Cr}(\text{CO})_5 \cdot \text{MeOH}$  complex is energized by a fluctuation in the local bath that allows for the removal of the solvating methanol molecule into the basins between the first and second solvent shells. The presence of a solvate in this space induces another to move into the same region. After diffusive motion within this long-lived state, the rearrangement is complete when the formally bound solvent molecule moves into the continuum, which leaves the other to bond to the metal fragment. While the present simulation suggests an  $I_d$  mechanism, the well defined order of the reactive steps shows mixed associative/dissociative dynamics occurring at the same reaction center. Thus, whether a particular ligand and metal fragment appear to rearrange according to a single traditional mechanism depends on whether the bottleneck of the reaction occurs in the first dissociative or second associative step. The reaction mechanism would appear to have a [metal fragment]-ligand bonding activating  $\Delta H^*$  and a positive  $\Delta S^*$  if the first dissociative process is the most important process in the mechanism. Likewise, if molecular diffusion of an exchanging ligand from the continuum into the normally void volume is the slow step, one would likely conclude that the mechanism is more associative in nature. Systems in which both processes are important would appear to undergo an interchange mechanism.

The present proposed mechanism accounts for many of the discrepancies observed in the reaction dynamics of ligand exchange in coordinatively unsaturated organometallic intermediates. While it may be true that every system of metal

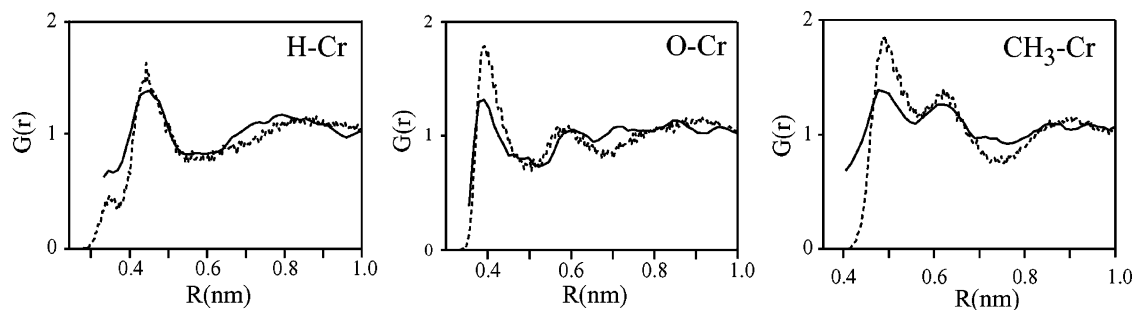


**Figure 5.** Radial distribution functions between the Cr metal center and the methanol solvent during the TPS simulations. Shown are the distribution functions for the second shell and beyond. The solid lines represent the nonequilibrium calculations which should be compared to the (dashed line) equilibrium results.

fragments and solvent molecules undergoes exchange from a mechanism that is unique to those interacting species, an  $I_d$  process with well-defined dissociative/associative dynamics unites many previous observations. Consequently, mechanistic and ultrafast experimental studies cannot capture the microscopic details of the reaction dynamics because the process is more complicated than a simple traditional mechanistic view allows. Further investigations of ligand rearrangement will focus on the nature of the transition states and rates of reaction from the stable to a possible metastable basin.

**B. Energetics.** Shown in Figure 3 is the total energy of the reacting molecules which represents the sum of the kinetic and potential energies of the two nearest exchanging methanol molecules and the organometallic fragment among themselves and with the remaining solvent bath. Also shown is the internal energy, which represents the sum of the kinetic energy and potential interactions only among the  $\text{Cr}(\text{CO})_5$  and two nearest methanol molecules. These data have been normalized such that the zero of energy represents the equilibrium value. It can be seen that the reactant species' internal energy rises above their total energy, the difference of which is the reactant/bath potential energetic coupling. The fact that the reactant/bath potential coupling dips below the equilibrium value suggests that the solvent acts to assist the exchange of ligands by providing extra internal energy into the reactive center. This interaction represents  $\sim 20\%$  of the internal energetics of the reaction as shown in Figure 3. This can be explained by dividing the Hamiltonian into reactant and bath contributions as expressed in eq 1. As the total energy is constant in the microcanonical ensemble ( $\Delta E = 0$ ), the change in total energy of the reactants (the two nearest methanol molecules and  $\text{Cr}(\text{CO})_5$  fragment) can be expressed as

$$\Delta E_{\text{reactants}} = -\Delta E_{\text{bath}} - \Delta V_{\text{reactant/bath}} \quad (2)$$

Consequently, if increasing the internal energy of the reactants ( $\Delta E_{\text{reactants}} \gg 0$ ) is necessary to crossover to the product basin, a decrease in both the energies of the bath and reactant/bath coupling is favorable to this process.

The observation of favorable transition state/bath coupling is in contrast to previous theoretical investigations of the  $\text{S}_{\text{N}}2$  reaction of  $\text{Cl}^-$  with  $\text{CH}_3\text{Cl}$ .<sup>35</sup> This study concluded that the

fast reaction is controlled by the instantaneous solvent configuration near the transition state. In our case, the long time scale of the transformation results in an adiabatic reaction mechanism in which the solvent has the time necessary to respond to the slow changes in the reactive basin. To test the generality of this phenomenon, the  $\text{S}_{\text{N}}2$  reaction of  $\text{Cl}^-$  with  $\text{CH}_3\text{Cl}$  has been simulated in the TPS ensemble. The initial results indicate that the fast displacement and charge switching result in unfavorable bath/reagent energies as had been observed in previous studies. Consequently, it is likely that our observations are representative of reactive systems in which the molecular nature of the reactants is not highly perturbed during the course of the reaction. Further studies of other reactive systems will be performed to ascertain the generality of these proposed dynamics.

## V. Conclusion

The present proposed mechanism accounts for the reaction dynamics of ligand exchange of coordinatively unsaturated organometallic intermediates. While it may be true that every system of metal fragments and solvent molecules undergoes ligand exchange from processes that are unique to those species, limiting forms of our proposed mechanism may account for a variety of conflicting conclusions concerning the mechanism of ligand exchange. Consequently, traditional mechanistic and ultrafast studies may not be able to capture the microscopic details of the dynamics. The internal energy of the reacting species by the bath through a favorable reactant/bath coupling assists the ligand exchange dynamics. This observation is likely due to the long time scale over which solvent exchange occurs as well as the fact that the molecular nature of the reacting species is intact throughout the course of the simulation.

**Acknowledgment.** We would like to thank T. McCormick for helpful discussions concerning the transition path sampling method and P. Geissler for critical reading of the manuscript. This work was supported by a grant from the National Science Foundation. We also acknowledge support from the Director, Office of Science, Chemical Sciences Division, under U.S. Department of Energy Contract DE-AC03-76SF00098.

JA044807T

(35) Bergsma, J. P.; Gertner, B. J.; Wilson, K. R.; Hynes, J. T. *J. Chem. Phys.* **1987**, *86*, 1356.